Nicotinamide mononucleotide (NMN) protects bEnd.3 cells against H₂O₂-induced damage via NAMPT and the NF-κB p65 signalling pathway

Xiujun Deng[1], Xinghuan Liang[2], Haiyan Yang[2], Zhenxing Huang[2], Xuemei Huang[2] (iD),
Chunfeng Liang[3], Yaqi Kuang[2], Yingfen Qin[2], Faquan Lin[1] and Zuojie Luo[2]

1 Department of Laboratory, The First Affiliated Hospital of Guangxi Medical University, Nanning, China
2 Department of Endocrinology, The First Affiliated Hospital of Guangxi Medical University, Nanning, China
3 Department of Blood transfusion, The First Affiliated Hospital of Guangxi Medical University, Nanning, China

An increasing number of studies have shown that nicotinamide mononucleotide (NMN) can inhibit not only ageing but also oxidative stress and inflammatory reactions by improving energy metabolism. However, the role of NMN in regulating the anti-apoptotic, antioxidative stress and inflammatory responses of brain microvascular endothelial cells is still unknown. Therefore, here we studied the effects of NMN on H₂O₂-induced oxidative damage of bEnd.3 cells. In this study, we found that NMN could inhibit the NF-κBp65 inflammatory signalling pathway and increase the expression of the enzymes NAMPT, VEGF and eNOS, alleviating H₂O₂-induced apoptosis in bEnd.3 cells. Taken together, these results suggest that NMN reduces H₂O₂-induced oxidative stress and apoptosis and improves cell functions by inhibiting the NF-κBp65 inflammatory pathway and increasing NAMPT expression.

Diabetes is a common disease. At present, the prevalence and incidence of diabetes have risen sharply worldwide.

Compared with nondiabetic patients, diabetic patients are more prone to stroke, and it has been reported that haemorrhagic stroke in diabetic patients is approximately 1.5 times that in nondiabetic individuals [1]. During the natural development of diabetes mellitus, endothelial cell dysfunction and the relative dysfunction of various endothelial mediators have generally been considered to be early signs of diabetic metabolic disorders. In turn, each metabolic disorder

(insulin resistance, compensatory hyperinsulinaemia, hyperglycaemia, oxidative stress, excessive free fatty acid release and lipotoxicity) occurring in diabetes mellitus may affect endothelial functions [2]. In the brain, endothelial cells are a specialized monolayer of cells arranged on the wall of the vascular lumen and constitute the most critical portion of the physical barrier between the blood and the brain called the blood–brain barrier (BBB) [3]. In the central nervous system, the BBB plays an important physiological role in regulating paracellular permeability, ion balance, nutrient transport and cerebral haemodynamics, and the

molecular characteristics of the BBB, adhesion junctions and transporters are particularly important [4,5]. The neurodegenerative changes caused by diabetes, obesity and Alzheimer's disease have similar pathways, including overlapping pathways of oxidative stress, mitochondrial dysfunction and inflammation, accompanied by impaired integrity of the blood–brain barrier [6].

Oxidative stress and inflammation are the key mediators of blood–brain barrier dysfunction. Abnormal metabolism and systemic inflammation lead to the excessive production of ROS in the brain and the release of inflammatory factors, which further lead to imbalances in endothelial cell regulatory protease and dysfunctional endothelial cell secretion [7,8]. Endothelial nitric oxide synthase (eNOs) and vascular endothelial growth factor (VEGF) are mainly involved in angiogenesis and changes in vascular permeability [9]. When vascular endothelial cells are affected by oxidative stress and other harmful factors, VEGF can activate many pathways, among which eNOS-induced impairments in the NO pathway are characteristics of impaired vascular endothelial function, which leads to a decrease in vasodilation factors, the expression of inflammatory factors and a decrease in angiogenesis [10,11]. A large amount of ROS produced by oxidative stress stimulate endothelial cells to express intercellular adhesion molecule (ICAM-1) and secrete matrix metalloproteinase (MMP), which attract and bind lymphocytes and monocytes in blood vessels, leading to inflammation [12]. In addition, oxidative stress also involves the activation of the NF-κB pathway, which controls the synthesis and release of the inflammatory factors interleukin-1 (IL-1) and tumour necrosis factor-α (TNF-α) [13] and further destroys the BBB.

NMN, as a direct enzymatic product of NAMPT, is a small molecule that can easily pass through the blood–brain barrier and mediate cell death, oxidative stress and inflammatory reactions under pathological conditions [14,15]. In recent years, increasing evidence has shown that NMN exerts a protective effect on cerebrovascular diseases and neuronal damage related to diabetes, ageing and oxidative stress, and these pathological processes often involve the reduction or depletion of NAD^+ [16,17,18]. Further studies showed that NMN has an anti-inflammatory effect and improves endothelial dysfunction induced by IL-1β or TNF-α, and this process is related to the regulation of intracellular NAD^+ levels by NMN in a manner dependent on the expression of CD78 on the surface of endothelial cells [19]. However, the impact of NMN on H_2O_2-induced oxidative stress and inflammation in bEnd.3 cells and changes in nampt levels remain unclear. Therefore, the aim of the present study was to investigate whether NMN inhibits H_2O_2-induced oxidative stress and inflammation in bEnd.3 cells and to determine the molecular mechanisms.

Materials and methods

Cell culture

bEnd.3 cells were purchased from Procell Life Science & Technology Co., Ltd. (Wuhan, China). bEnd.3 cells were maintained at 37°C in a humidified atmosphere of 5% CO_2 and 95% air in DMEM containing 10% heat-inactivated fetal bovine serum (Gibco, Grand Island, NY, USA), 50 $U \cdot mL^{-1}$ penicillin and 50 $mg \cdot mL^{-1}$ streptomycin (Solarbio, Beijing, China).

Preparation and treatment with NMN

Nicotinamide mononucleotide was purchased from Sigma-Aldrich (St. Louis, MO, USA). NMN was prepared as a stock solution in double-distilled water and was diluted to the final concentration before the experiment. The prepared stock solution of 10mM NMN was stored at −20 °C.

Cell viability assay

bEnd.3 cells were treated with different concentrations of H_2O_2 (0, 500, 700, 800, 900 and 1000 μM) and NMN (0, 100, 200, 300, 500 and 600 μM) for 24 h. Then, bEnd.3 cells were treated with 100 μL of DMEM and 10 μL of Cell Counting Kit-8 Reagent (AbMole BioScience, Inc., Houston, TX, USA). The plates were incubated in the dark for 1 h at 37°C. The optical density (OD) value was measured using a Synergy H1 Reader (BioTek, Winooski, VT, USA) at 450 nm.

Apoptosis analysis

bEnd.3 cells were collected by trypsinization, washed twice with cold PBS and then resuspended in 1x binding buffer, which is a buffer containing Ga^+. Then, 100 μL of the solution was transferred to a 5-ml culture tube before being incubated with 5 μL of Annexin V-FITC and 5 μL of PI (BD Biosciences, Franklin Lakes, NJ, USA) in the dark for 25 min at room temperature. Stained cells were detected by flow cytometry (BD Biosciences) within an hour.

Apoptotic cells were also analysed by Hoechst 33258 staining. After the appropriate treatments, bEnd.3 cells were fixed with 4% paraformaldehyde for 20 min; then, the 4% paraformaldehyde was removed, the cells were rinsed with PBS three times, and Hoechst 33258 (Beyotime, Shanghai, China, 500 μL/well) was added and incubated for 20–30 min. The images were captured under a fluorescence microscope (Nikon Corporation, Tokyo, Japan).

Apoptotic dying cells were identified as the cells with blue fragmented, condensed nuclei, and the percentage of apoptotic bEnd.3 cell was calculated as from total number of cell population. The percentage of apoptotic cells was analysed by Image J software.

Measurement of $\Delta\Psi m$

After experimental treatments, the cells were incubated with JC-1 (Beyotime) staining solution at 37 °C for 20 min and then resuspended in 500 µL of precooled JC-1 staining buffer. Fluorescence microscopy (Nikon Corporation, Tokyo, Japan) was used to obtain the photographs of the cells. The complexes with red fluorescent were formed in cells with normal mitochondria. In mitochondria-damaged cells, JC-1 maintained a monomeric form and showed green fluorescence. The ratio of red to green light in the obtained photographs was quantitatively analysed by ImageJ software.

ROS level measurement

Treated cells were washed with PBS and incubated with serum-free basal medium, which contained 2,7-dichlorodihydrofluorescein diacetate (DCFH-DA, Beyotime), for 20–30 min at 37°C in the dark. The cells were washed with serum-free cell culture solution, and then, the fluorescence intensity in the cells, which represented ROS production, was measured by immunofluorescence microscopy (Nikon Corporation, Tokyo, Japan) at an excitation wavelength of 488 nm and an emission wavelength of 525 nm.

Detection of catalase (CAT) and superoxide dismutase (SOD) activity

The activities of the antioxidant enzymes, catalase (CAT) and superoxide dismutase (SOD) were measured using the Catalase Assay Kit (Nanjing Jiancheng Bioengineering Research Institute, Nanjing, China) and Micro-method SOD Activity Detection Kit (Solarbio, Beijing, China). Every 5 million cells were mixed with 1 mL PBS or superoxide dismutase lysis buffer, lysed by ultrasound and then centrifuged at 8000 g for 10 min at 4 °C, and the supernatant was taken for detection. The absorbance of CAT and SOD was measured on Synergy H1 Reader (BioTek) with wavelengths of 560nm and 405 nm, respectively, and the result was expressed as $U \cdot mg^{-1}$ protein.

Determination of lactate dehydrogenase (LDH) and caspase-3

The effect of NMN on cell cytotoxicity was determined using the Spectrophotometric LDH Determination Kit (Solarbio, Beijing, China). The cells were added 1 mL

LDH extract to be sonicated (ultrasound for 3 s, 10-s interval, repeated 30 times) and then centrifuged at 8000 g at 4 °C for 10 min, and the supernatant was measured on Synergy H1 Reader (BioTek) at 450nm absorbance. The result was expressed as $U \cdot mg^{-1}$ protein. In addition, Colorimetric Caspase-3 Activity Assay Kit (Solarbio) was used to determine caspase-3 activity. The cells were lysed by shaking with 200 µL caspase-3 lysis solution, ice-bathed for 10 min, shaken again and then centrifuged at 12 000 g at 4 °C for 10 min, and the supernatant was taken to determine the OD value at 405nm using Synergy H1 Reader (BioTek). The percentage increase in caspase activity was expressed by the following formula: 100%×[(experimental treatment group OD - blank control OD)/(experimental control OD - blank control OD)].

Reverse transcription–quantitative polymerase chain reaction (RT–qPCR)

The RNA purity was determined after extracting the total RNA from cells using NucleoZOL Reagent (Macherey-Nagel, Düren, Germany) according to the manufacturer's protocols. Oligo-dT primers and AMV reverse transcriptase (Takara, Shiga, Japan) were used to synthesize cDNA. Amplification of the cDNA was performed using the FastStart Universal SYBR Green Master Mix (Roche, Mannheim, Germany) on an ABI StepOnePlus (Applied Biosystems, Boston, MA, USA). The primer sequences used are listed in Table 1. GAPDH was used as an internal reference. The quantification of gene expression was performed using the $2^{-\Delta\Delta Ct}$ method.

Western blot analysis

The cells were cultured with H_2O_2 (800 µM) and pretreated with NMN (300 µM) for 24h, and then, cells were lysed with radioimmunoprecipitation assay buffer (Solarbio) to obtain total protein extracts or used Nuclear and Cytoplasmic Extraction Kit (Shanghai Ya Enzyme Biotechnology Co., Ltd, Shanghai, China) to extract nuclear protein. Subsequently, the protein concentration was determined using a BCA Protein Analysis Kit (Beyotime Institute of Biotechnology). The proteins were separated by SDS/PAGE (Bio-Rad, Hercules, CA, USA, USA) and then transferred onto a PVDF membrane (Millipore, Billerica, MA, USA), which was incubated with 5% nonfat dry milk TBST. The protein-containing membrane was incubated with anti-NF-κB p65, anti-IL-1, anti-TNF-α, anti-ICAM-1, anti-MMP9 (Cell Signaling Technology, Danvers, MA, USA, Cat. No. 3033, Cat. No. 12507, Cat. No. 11948, Cat. No. 67836, Cat. No. 13667), anti-NAMPT (Abcam, Cambridge, UK, Cat. No. 236874), anti-GAPDH and anti-PCNA (Signalway Antibody, Nanjing, China, Cat. No. 21612, Cat. No. 29168) antibodies at 4 °C overnight. Then, the membrane was

Table 1. Sequences of the primers employed for reverse transcription–quantitative polymerase chain reaction

Name	Forward primer(5′–3′)	Reverse primer(5′–3′)
NF-KBp65	TCGAGTCTCCATGCAGCTACGG	CGGTGGCGATCATCTGTGTCTG
Nampt	CGCAAGAGACTGCTGGCATAGG	ACTGTGCTCTGCTGCTGGAAC
IL-1β	TCGCAGCAGCACATCAACAAGAG	TGCTCATGTCCTCATCCTGGAAGG
ICAM-1	CTGAAAGATGAGCTCGAGAGT	AAACGAATACACGGTGATGGTA
MMP-9	CAAAGACCTGAAAACCTCCAAC	GACTGCTTCTCTCCCATCATC
VEGF	TAGAGTACATCTTCAAGCCGTC	CTTTCTTTGGTCTGCATTCACA
ENOs	CTGAGAGCCTGCAATTACTACC	TTTCCACAGAGAGGATTGTAGC
TNF-α	ATGTCTCAGCCTCTTCTCATTC	GCTTGTCACTCGAATTTTGAGA
GAPDH	TGCTGTCCTGTATGCCTCTG	TTGATGTCACGCACGATTTCC

incubated with horseradish peroxidase-conjugated secondary antibodies (Signalway Antibody, Cat. No. L3012) for 1 h at 37°C. Subsequently, the proteins were confirmed by visualization using a LI-COR system (Odyssey, Lincoln, NE, USA) according to the manufacturer's instructions. The intensity of the bands of interest was analysed with ImageJ software version 1.8.0.

Statistical analysis

Graphs were generated using GraphPad Prism 6.0 (GraphPad Software Inc., San Diego, CA, USA) and ImageJ 1.8.0 (National Institutes of Health, USA). The results are expressed as the mean $\pm$ SD and were analysed with SPSS 17.0 software. One-way ANOVA was selected to analyse the differences among the groups. A value of $P < 0.05$ was considered statistically significant.

Results

NMN protects cells from H_2O_2-induced decline in proliferation activity

To investigate the effects of NMN and H_2O_2 on the viability of bEnd.3 cells, a CCK-8 Kit was used to measure cell proliferation rate. The results showed that the cells were exposed to 800 μM H2O2 for 24h, the survival rate of the cells decreased by about 50% compared with the control group, while 50, 100 and 300 μM NMN for 24 h significantly improved cell proliferation rate compared with the control group (Fig. 1A.B); furthermore, bEnd.3 cells were damaged by 800 μM H_2O_2 after pretreatment with 50, 100, 300 and 500 μM NMN for 24 h, and it was observed that 50–300 μM NMN significantly increased cell proliferation rate compared with the that of the H_2O_2 group ($P < 0.05$), and no significant differences were observed among the 50–300 μM NMN groups; however, the effect of 500 μM NMN on cell viability was not different from that of the H_2O_2 group (Fig. 1C).

NMN reduces H_2O_2-induced bEnd.3 cell apoptosis

To determine whether NMN improved cell viability by suppressing H_2O_2-induced cell apoptosis in bEnd.3 cells, the rate of apoptosis was evaluated by flow cytometry. The results showed that after incubation with 800 μM H_2O_2 for 24 h, the apoptosis rate was increased compared with that of the control group, while NMN (50, 100, 200, 300 and 400 μM) reduced the apoptosis rate compared with that of the H_2O_2 group ($P < 0.05$); however, 500 μM NMN did not affect apoptosis ($P > 0.05$) (Fig. 2). These results suggest that the effect of NMN on bEnd.3 cell apoptosis in vitro was consistent with the results of the CCK-8 assay.

Hoechst 33258 staining was further used to show that NMN alleviated H_2O_2-induced early apoptosis in bEnd.3 cells. After bEnd.3 cells were pretreated with 300 μM NMN for 24 h, the number of bright blue fluorescent cells was significantly reduced, indicating that NMN can significantly reduce the apoptotic cells and nuclear concentration caused by H_2O_2 (Fig. 3A,B). In addition, the cells in the H_2O_2 treatment group grew slowly, lost the appearance of paving stones, changed their morphology and were flat; the number of adherent cells decreased compared with that of the control group; and 300 μM NMN reversed these changes (Fig. 3C).

Effect of H_2O_2 on the mitochondrial membrane potential of bEnd.3 cells

Oxidative stress and inflammation-induced decreases in mitochondrial membrane potential are markers of early cell apoptosis. Changes in mitochondrial membrane potential were determined by JC-1 staining. The results showed that the red fluorescence of H_2O_2-induced cells decreased, the green fluorescence increased, and the ratio of red-to-green fluorescence decreased significantly compared with those of the control group (Fig. 4A,B), indicating that mitochondrial membrane
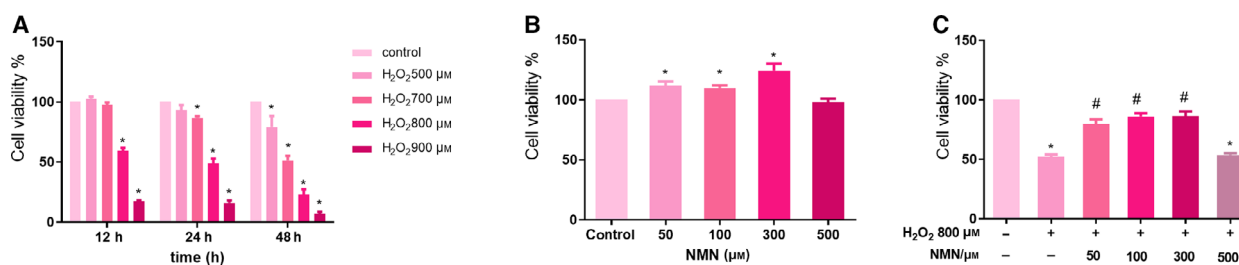
Fig. 1. NMN alleviates decreased viability of bEnd.3 cells induced by H_2O_2. A-B. bEnd.3 cells were exposed to different times (12, 24, 48 h) and various concentrations of H_2O_2 (0, 500, 700, 800, 900 μM) and NMN (50, 100, 300, 500 μM) for 24 h. C. NMN pretreated cells with 800 μM H_2O_2 to induce damage. Results are expressed as means ± SD and are representative of three independent experiments. Data were analysed by one-way ANOVA with LSD's test for multiple comparisons. *$P < 0.05$, vs. control group. #$P < 0.05$, vs. 800 μM H_2O_2 group.

potential decreased. After NMN treatment, the red-green fluorescence ratio increased, indicating that the mitochondrial membrane potential increased.

Effect of NMN on ROS levels in bEnd.3 cells damaged by H_2O_2

The fluorescent probe DCFH-DA can be used to detect reactive oxygen species; reactive oxygen species in cells can oxidize nonfluorescent DCFH to generate fluorescent DCF, and the fluorescence intensity represents the level of reactive oxygen species in cells. There were significant differences in the relative fluorescence intensities among the control group, oxidative damage group and NMN 300 μM group. Compared with that of the control group, the relative fluorescence intensity of the oxidative damage group was significantly enhanced, and a large amount of ROS was produced in the oxidative damage group. Compared with the oxidative damage group, the 300 μM NMN group exhibited significantly reduced ROS induced by H_2O_2. However, NMN alone had no effect on ROS levels in cells (Fig. 5A,B).

NMN increases the activities of CAT and SOD in H_2O_2-treated bEnd.3 cells

To investigate whether NMN mediates antioxidant enzyme activity to protect bEnd.3 cells from H_2O_2-induced apoptosis, we measured the activities of CAT and SOD. When bEnd.3 cells were treated with 800 μM H_2O_2, the activities of SOD and CAT in the cells were significantly decreased compared with the control group, whereas pretreatment with 300 μM NMN significantly increased the activities of CAT and SOD compared with the H_2O_2 treatment group ($P < 0.05$) (Fig. 5C,D).

NMN reduces the elevation of LDH and caspase-3 in bEnd.3 cells under H_2O_2 conditions

After the cells were pretreated with NMN and then treated with H_2O_2 for 24h, the cytotoxicity was determined by measuring the level of LDH. The results showed that the cytotoxicity of the cells in the H_2O_2 treatment group increased compared with control group ($P < 0.05$) and the cell cytotoxicity decreased in H_2O_2 + NMN group compared with H_2O_2 group ($P < 0.05$) (Fig. 5E). In addition, we also measured the activity of caspase-3, and the results showed that bEnd.3 cells treated with H_2O_2 significantly increased caspase-3 compared with the control group, while caspase-3 after NMN pretreatment significantly decreased compared with the H_2O_2 treatment group ($P < 0.05$) (Fig. 5F). The above showed that NMN inhibited H_2O_2-induced cytotoxicity and caspase-3 activation to reduce bEnd.3 cell apoptosis.

Effect of H_2O_2 and NMN on the expression of genes associated with the NF-κB p65 inflammatory pathway

We further examined the effect of NMN on the expression of function-related factors and NF-κB inflammatory pathway factors in bEnd.3 cells under hydrogen peroxide stimulation. RT-qPCR confirmed that NMN inhibited the H_2O_2-induced increase in the NF-κB inflammatory pathway factors (TNF-α, IL-1, ICAM-1 and MMP9). Moreover, NMN restored NAMPT, eNOS and VEGF expression, which were reduced by H_2O_2, to normal levels, and compared with the control group, NMN alone increased the levels of NAMPT, eNOS and VEGF. Moreover, the administration of NMN suppressed the NF-κBp65 inflammatory pathway and restored endothelial cell-related functional factors upon H_2O_2 exposure (Fig. 6).
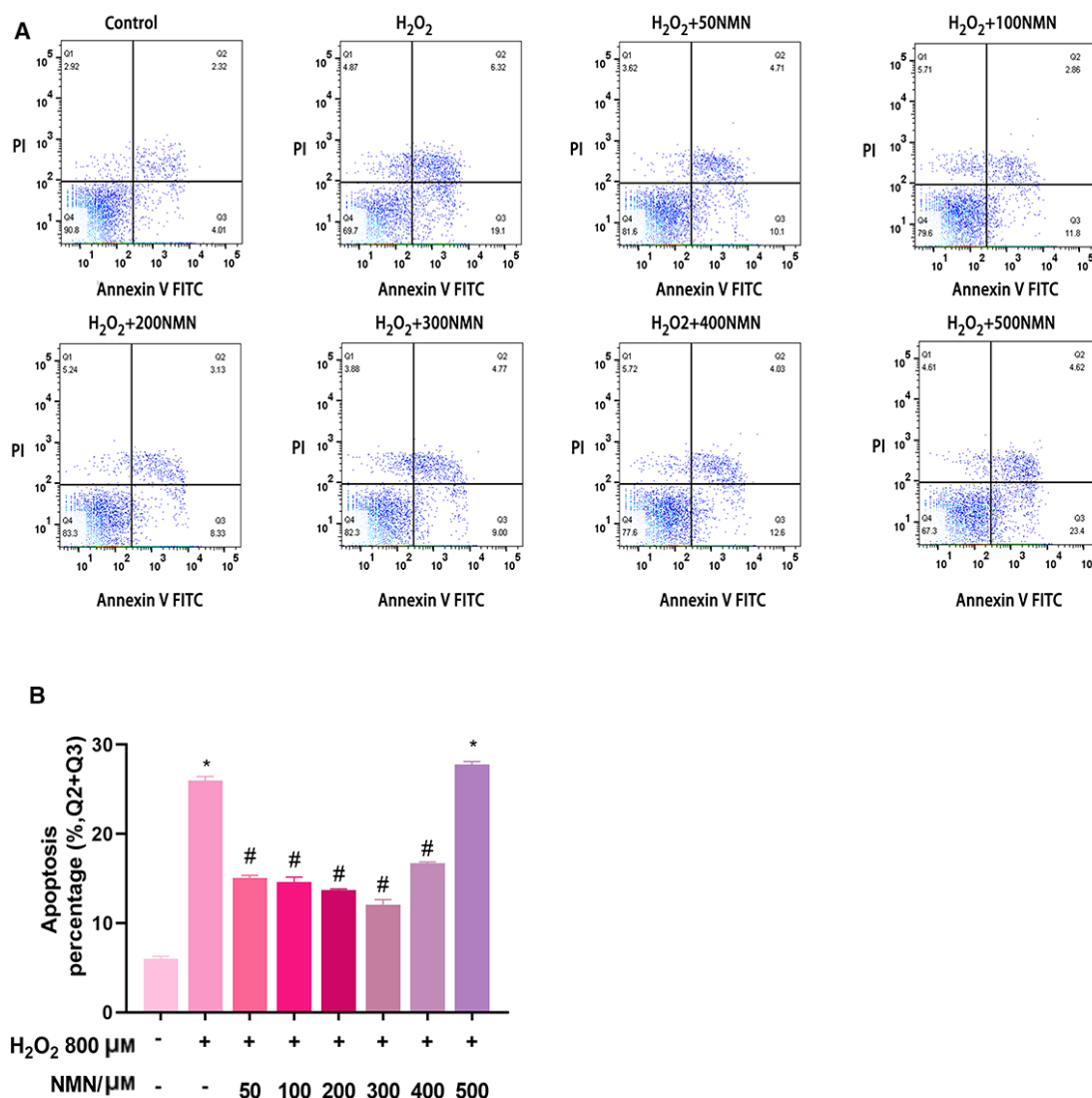
Fig. 2. (A) Early and late apoptotic events in bEnd.3 cells injured by H_2O_2 and the effects of various concentrations of NMN on 800 μM H_2O_2-induced apoptosis were detected by flow cytometry. The top left quadrant indicates nonapoptotic cells; the top right quadrant represents late apoptotic events; the bottom right quadrant represents early apoptotic cells; and the bottom left quadrant represents living cells. B. The apoptosis rate of bEnd.3 cells induced by H_2O_2 that were pretreated with different concentrations of NMN was analysed by FLOWJO software. Results are expressed as means ± SD and are representative of three independent experiments. Data were analysed by one-way ANOVA with LSD's test for multiple comparisons. *$P < 0.05$, #$P < 0.05$ vs. the control group. #$P < 0.05$ vs. the 800 μM H_2O_2 group.

Effects of NMN on the activity of NAMPT and the expression of NF-κB p65, IL-1, TNF-α, MMP9 and ICAM-1 in oxidative stress-injured bEnd.3 cells

NAMPT is a secreted cellular enzyme that participates in stress reactions, such as inflammation, under pathological conditions to avoid apoptosis [20]. Transcription of the proinflammatory cytokines IL-1β, TNF-α and ICAM-1 is mainly regulated by the NF-κB pathway. Activated IL-1β and TNF-α promote endothelial cells to express MMP9 and further exacerbate inflammatory reactions [21,22]. We further examined the inflammatory signalling pathway to verify the protective effect of NMN on bEnd.3 cells under oxidative stress. As shown in Fig. 6, the expression levels of NF-κB p65, MMP9, ICAM-1, TNF-α and IL-1β were markedly higher in the H_2O_2 groups than in the control group ($P < 0.05$), but the level of NAMPT decreased significantly ($P < 0.05$). Additionally,
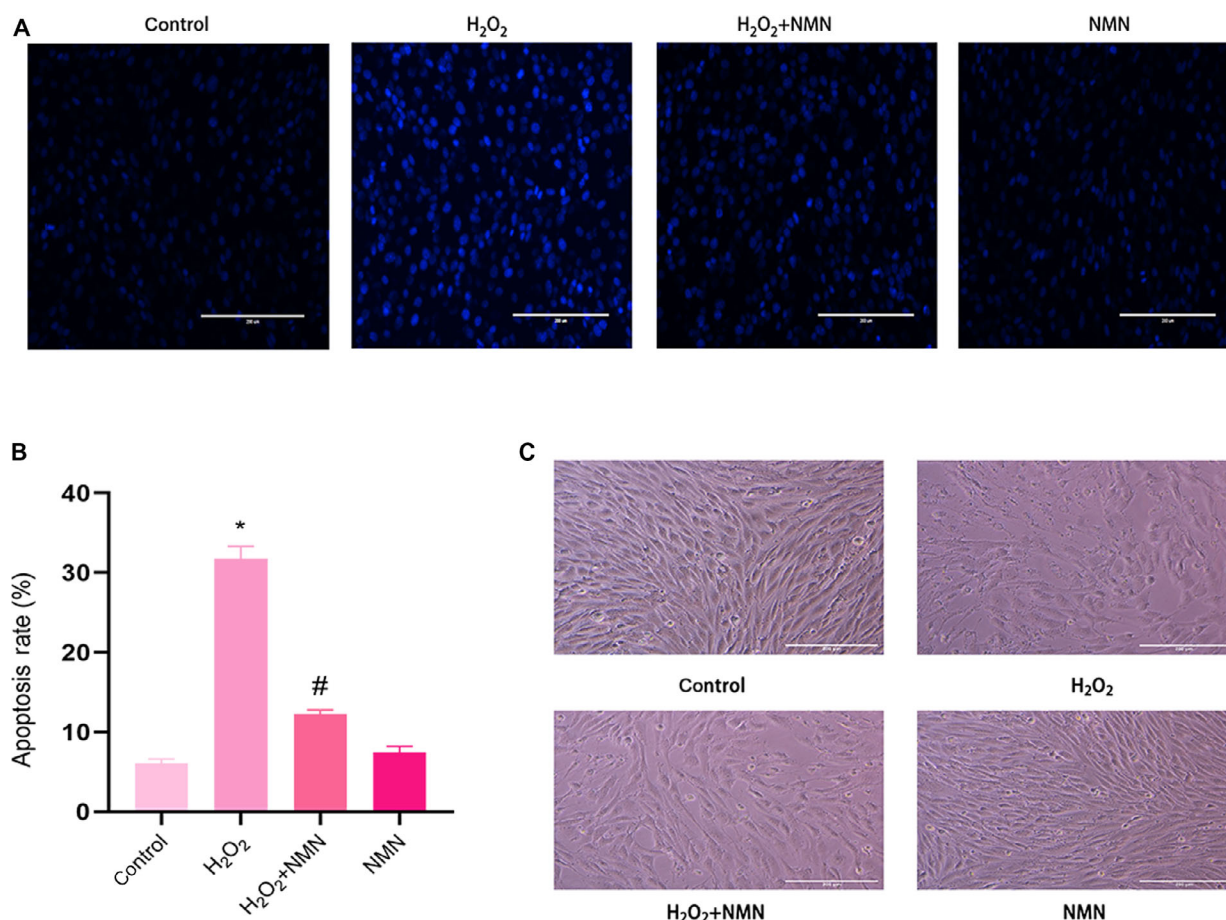
Fig. 3. (A) Apoptosis of cells that induced by H_2O_2 (800 μM) and NMN (300 μM) reduced apoptosis induced by H_2O_2 was stained with Hoechst 33258. (B) The apoptotic and total cells were analysed by IMAGEJ software, and the apoptosis rate was presented as % of the total number of nuclei C. bEnd.3 cells were cultured with 800 μM H_2O_2 and 300 μM NMN (×10 scale bar = 100 μm). Results are expressed as means ± SD and are representative of three independent experiments. Data were analysed by one-way ANOVA with LSD's test for multiple comparisons. *$P < 0.05$, #$P < 0.05$ vs. control group. #$P < 0.05$, vs. 800 uM H_2O_2 group.

compared with that of the H_2O_2 group, the expression of NF-κB p65, MMP9, ICAM-1, TNF-α and IL-1β was inhibited in the H_2O_2 + NMN group; the protein expression levels of NAMPT notably and significantly increased (Fig. 7 A–F). Compared with the control group, NMN alone significantly increased the protein level of NAMPT and inhibited the expression of NF-κB p65 ($P < 0.05$). The results of the present study suggested that the enzyme NAMPT and NF-κB p65 signalling were associated with the protective effects of NMN on H_2O_2-induced bEnd.3 cells.

Discussion

Diabetic cerebral microangiopathy mainly manifests as damage to the blood–brain barrier, which leads to the dysfunction of vascular endothelial cells.

Neurovascular coupling leads to hypoxia-induced activation of transcription factors, which in turn triggers inflammation and enhances vascular permeability, and studies have shown that the onset of microvascular disease may occur earlier than the onset of type 2 diabetes [23,24]. Since the blood–brain barrier is mainly composed of vascular endothelial cells, we used bEnd.3 cells to establish a blood–brain barrier model in our experiments. It is generally accepted that oxidative stress and inflammation are key factors that cause endothelial cell dysfunction and increased vascular permeability [25,26]. Treatment with high concentrations of H_2O_2 can cause oxidative stress, inflammation and even apoptosis [27]. Exposure to H_2O_2 is a simple and effective in vitro cell model to study oxidative stress-induced damage in diabetic brain microvascular endothelial cells. Therefore, in the current study, H_2O_2
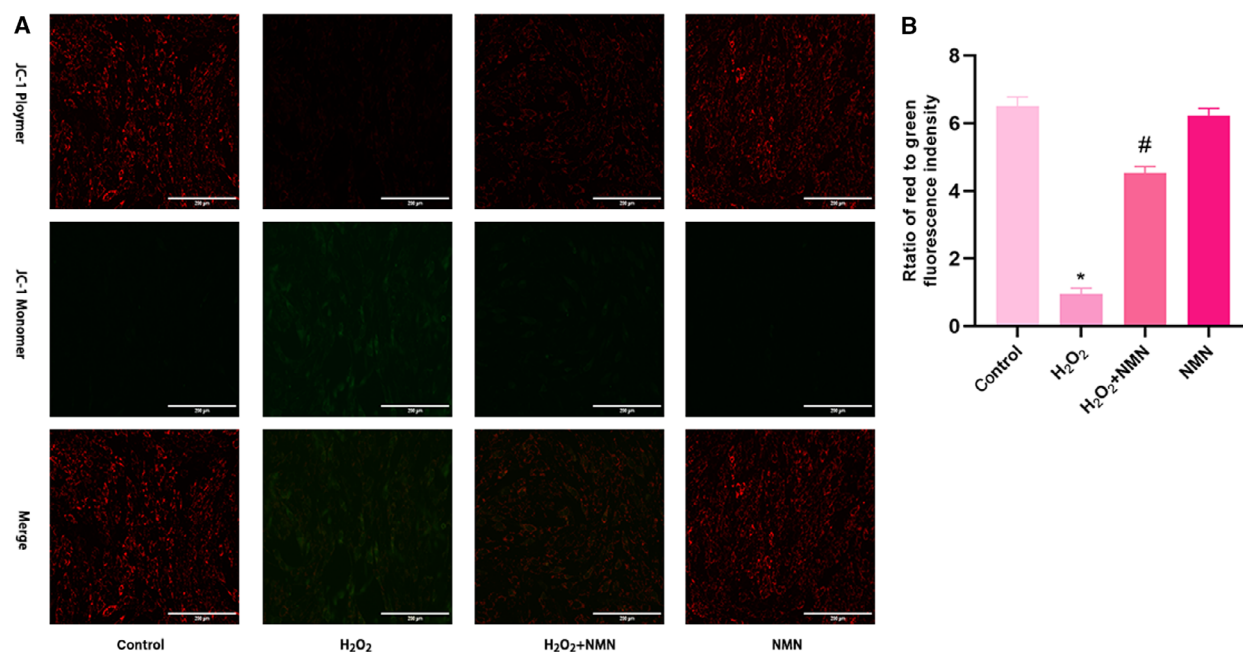
Fig. 4. Protective effect of NMN (300 µM) on mitochondrial damage induced by H_2O_2 (800 µM). (A) Immunofluorescence microscopy of mitochondrial membrane potential shown by JC-1 staining (×20; scale bar = 200 µm). (B) The ratio of red-green fluorescence intensity indicating the mitochondrial membrane potential by JC-1 staining. Results are expressed as means ± SD and are representative of three independent experiments. Data were analysed by one-way ANOVA with LSD's test for multiple comparisons. *$P < 0.05$ vs. the control group. #$P < 0.05$ vs. the H_2O_2 group.

was selected to induce oxidative stress damage in bEnd.3 cells. We first screened the concentration of H_2O_2 with CCK-8 assays, and the results showed that 800 µM H_2O_2 had the best inhibitory effect on cell viability after 24 h. The H_2O_2 concentration in our experiment was different from the concentration used in other literatures, which might be due to the cell growth status and other external experimental conditions and methods. However, after our repeated verification, 800 µM H_2O_2-induced bEnd.3 cells were an effective and stable model of oxidative stress in our experiments.

Increasing evidence has shown that NMN has beneficial effects on various physiological functions and therapeutic significance in diabetes, obesity, cardiovascular diseases and other disease models [28]. Kiss T et al [29,30] suggested that NMN treatment in vivo in ageing rats and in vitro in brain microvascular endothelial cells from aged rats could improve mitochondrial oxidative stress, inflammation, endothelial cell dysfunction and prevent neurovascular coupling (NVC) reactions. In addition, Stefano Tarantini et al. [18] found that NMN supplementation increased endothelial NO-mediated vasodilation to rescue the NVC response in elderly rats and could reduce mitochondrial oxidative stress and

H_2O_2 release in elderly brain microvascular endothelial cells. Caton PW et al [31] reported that NMN could correct islet dysfunction induced by inflammatory factors, possibly by inhibiting the expression of genes such as IL-1β and TNF-α, and inhibit the nitric oxide enzyme. In the present study, it was suggested that NMN exerted a protective effect against H_2O_2-induced oxidative damage in bEnd.3 cells. In the present study, the results showed that NMN (50, 100 and 300 µM) significantly increased the viability of bEnd.3 cells, indicating that NMN could induce cell survival; then, the effects of NMN on H_2O_2-induced cell viability and apoptosis were measured by CCK-8 assays, Hoechst 33258 and flow cytometry. The findings at this stage suggested that NMN protected cells from H_2O_2-induced damage by increasing cell vitality. We also measured LDH activity, which further verified the toxic effect of H_2O_2 on bEnd.3 cells and the protective effect of NMN on cells. In addition, under the microscope, it was found that the cell volume of the H_2O_2 group shrank, the shape was irregular, the cells were significantly reduced and there were many necrotic cells compared with the control group, while the NMN pretreatment group had fuller cell shape and increased adherent cells compared with the H_2O_2 group.
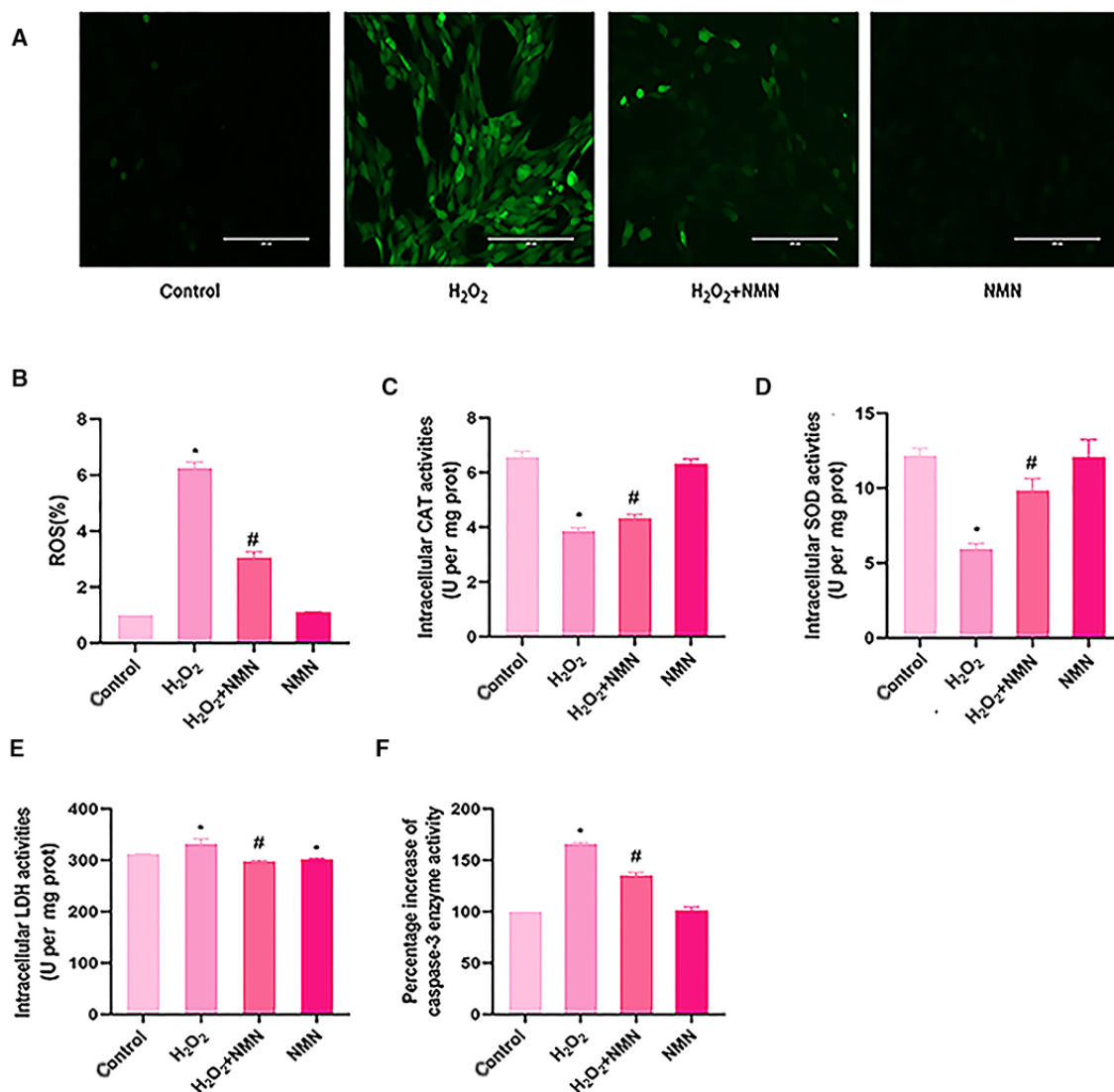
Fig. 5. Nicotinamide mononucleotide decreased intracellular ROS, LDH and caspase-3 level but increased CAT and SOD activities treated with H_2O_2. bEnd.3 cells were pretreated with 300 μM NMN for 24 h and then exposed to 800 μM H_2O_2. (A) ROS was measured by the fluorescent probe DCFH-DA and imaged by fluorescence microscopy (×20; scale bar = 200 μm). (B) The average fluorescence intensity was calculated by ImageJ software and reflects the intracellular ROS level. C-F. The activities of cellular CAT, SOD, LDH and caspase-3. The CAT, SOD and LDH levels were normalized per milligram of protein. The level of caspase-3 was expressed as the percentage increase in activity compared with the normal group. Results are expressed as means ± SD and are representative of three independent experiments. Data were analysed by one-way ANOVA with LSD's test for multiple comparisons. *$P < 0.05$, #$P < 0.05$ vs. the control group. #$P < 0.05$ vs. the H_2O_2 group.

Oxidative stress refers to the imbalance in oxidation and antioxidation in the body, which tends to oxidize substances, leading to the inflammatory infiltration of neutrophils, increased secretion of proteases and the production of a large number of key oxidation products. ROS are mainly derived from mitochondria and are an important part of the regulatory transduction pathway; when ROS exceed the antioxidant capacity

of the cell, they pose a continuous threat to the cell, resulting in a condition called oxidative stress [32,33]. Evidence has suggested that NMN treatment can improve mitochondrial oxidative stress and apoptosis in nucleus pulposus cells induced by advanced glycation end products (AGEs) [34]. Wang X et al [35] confirmed that NMN attenuated and eliminated neuronal death and ROS accumulation in rat hippocampal slices
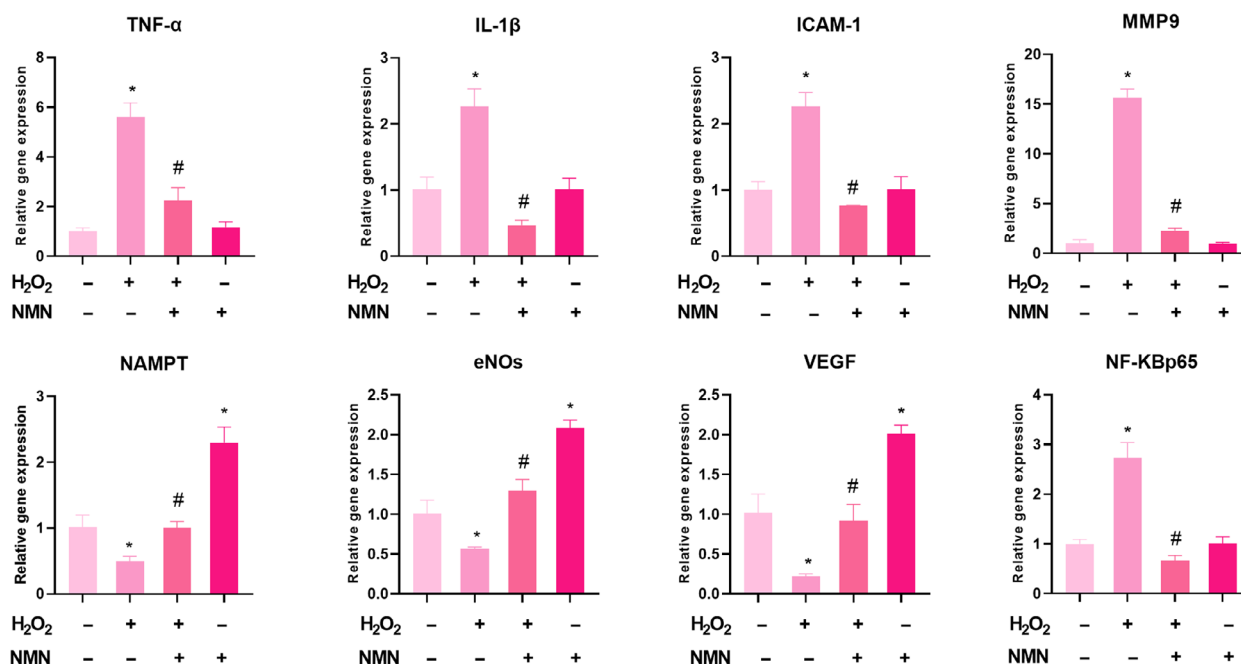
Fig. 6. mRNA expression levels of TNF-α, IL-1β, ICAM-1, MMP-9, NAMPT, eNOs, VEGF and NF-KBp65 were detected by reverse transcription–quantitative polymerase chain reaction. Results are expressed as means ± SD and are representative of three independent experiments. Data were analysed by one-way ANOVA with LSD's test for multiple comparisons. *$P < 0.05$, vs. control group. #$P < 0.05$, vs. H_2O_2 group.

treated with Aβ1-42 oligomers. CAT is a common enzyme that reacts effectively with hydrogen peroxide, and its catalytic activity decomposes hydrogen peroxide into oxygen and water, SOD is an antioxidant enzyme, which plays a central role in neutralizing O2, and when oxidative stress comes, CAT and SOD together form the main line of defence against superoxide radicals and ROS [36]. In order to verify whether endothelial cell damage is related to oxidative stress, the content of ROS and the activity of antioxidant enzymes were measured. In the present study, we confirmed that NMN pretreatment significantly reduced the production of ROS induced by H_2O_2 and increased the activity of CAT and SOD. Therefore, NMN could protect bEnd.3 cells from cell damage caused by oxidative stress.

Cytochrome C is also an apoptosis-promoting protein that can induce apoptosis by activating caspase family, in caspase cascade reaction, apoptosis effector caspase-3 can be activated by cytochrome C and eventually lead to cell apoptosis [37]. We detected the activity of caspase-3 and found that compared with the control group, the activity of caspase −3 in bEnd.3 cells was increased by H_2O_2 treatment, but decreased by 300 μM NMN treatment, which proved that NMN played an anti-apoptosis role by blocking the activation of caspase −3.

When oxidative stress occurs, the activation of the transcription factor NF-κB p65 causes the activation of cellular inflammatory factors, resulting in high expression of IL-1β and TNF-α, while the leucocyte adhesion molecule ICAM-1 and inflammatory factors promote and form a malignant cycle [38]. Regarding vascular endothelial function, studies have confirmed that eNOS signal transduction regulated by VEGF is essential for endothelial cell proliferation and proper angiogenesis [39]; in addition, studies have shown that increased vascular permeability often results in high expression of MMP9 [40]. Our results showed that NMN effectively prevented H_2O_2-induced apoptosis by increasing ΔΨm, downregulating NF-κB p65, IL-1β, TNF-α, ICAM-1 and MMP9, and upregulating VEGF and eNOS expression. These findings indicate that NMN stabilized endothelial cell function and inhibited apoptosis mediated by the NF-κB p65 inflammatory pathway, thereby protecting bEnd.3 cells from apoptosis.

NAMPT enzyme is expressed in almost all organs and mainly has two forms: intracellular (iNAMPT) and extracellular (eNAMPT), among which iNAMPT mainly exists in cytoplasm and nucleus [41]. According to previous reports, NAMPT plays a multidirectional role in vascular homeostasis by regulating the functions of endothelial cells, vascular smooth muscle cells,
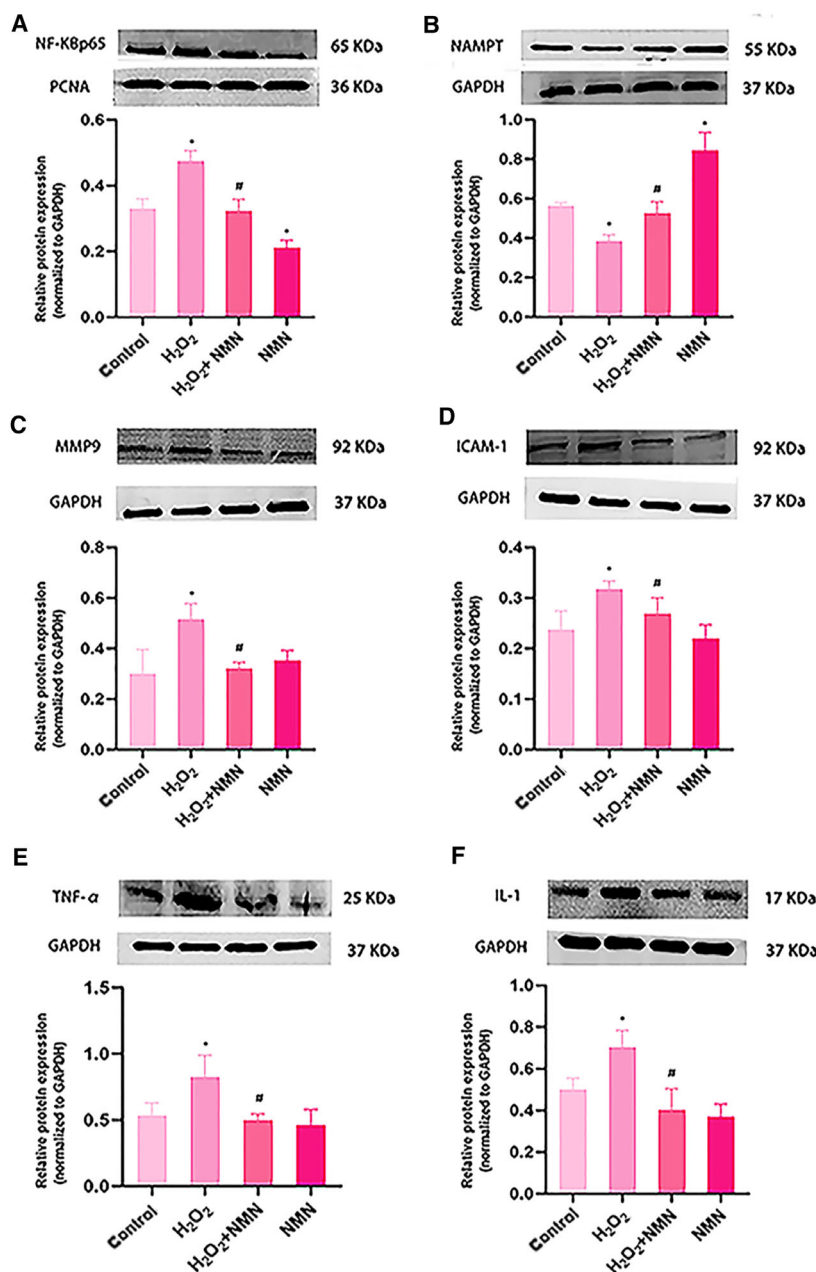
Fig. 7. Expression levels of the MMP9, nampt and NF-KBp65 signalling-related proteins, TNF-α, IL-1β and ICAM-1 after H_2O_2 and NMN treatment in bEnd.3 cells (A–F). Results are expressed as means ± SD and are representative of three independent experiments. Data were analysed by one-way ANOVA with LSD's test for multiple comparisons. *$P < 0.05$ vs the control group ; #$P < 0.05$, vs. H_2O_2 group.

endothelial progenitor cells and perivascular cells [42], and the overexpression of NAMPT can increase proliferation and prolong replication even under high glucose conditions by delaying ageing markers and limiting the accumulation of reactive oxygen species (ROS) [43]. In our study, it was found that the expression levels of NAMPT in bEnd.3 cells were significantly decreased after 800 μM H_2O_2-induced injury and could be reversed by NMN treatment. It is worth noting that when bEnd.3 cells were treated with NMN alone, the gene expression levels of NAMPT, eNOs and VEGF

were significantly increased compared with those of the control group, which was consistent with the fact that NMN could increase cell viability, and NMN treatment upregulated NAMPT and downregulated NF-κB p65 protein expression. The results showed that NMN improved H_2O_2-induced bEnd.3 cell apoptosis not only by inhibiting the NF-κB p65 inflammatory pathway but also by upregulating the enzyme NAMPT, which may have a certain antagonistic effect.

Taken together, our results demonstrate that NMN is capable of protecting H_2O_2-injured bEnd.3 cells

from apoptosis through the regulation of the enzyme NAMPT and the NF-κB p65 signalling pathway.

Acknowledgements

Conflict of interest

The authors declare no conflict of interest.

Author contribution

ZL and XL designed the experiment and provided the financial support; XD and CL, and YQ conducted the experiment; XD wrote the manuscript; and all authors contributed to data analysis.

Data accessibility

Upon reasonable request, the corresponding author will provide data.

References

1 Umemura T, Kawamura T and Hotta N (2017) Pathogenesis and neuroimaging of cerebral large and small vessel disease in type 2 diabetes: a possible link between cerebral and retinal microvascular abnormalities. *J Diabet Investigat* **8**, 134–148.

2 Coco C, Sgarra L, Potenza MA, Nacci C, Pasculli B, Barbano R, Parrella P and Montagnani M. (2019) Can epigenetics of endothelial dysfunction represent the key to precision medicine in type 2 diabetes mellitus? *Int J Mol Sci* **20**, 2949.

3 Lutton EM, Farney SK, Andrews AM, Shuvaev VV, Chuang GY, Muzykantov VR and Ramirez SH (2019) Endothelial targeted strategies to combat oxidative stress: improving outcomes in traumatic brain injury. *Front Neurol* **10**, 582.

4 Abdullahi W, Tripathi D and Ronaldson PT (2018) Blood-brain barrier dysfunction in ischemic stroke: targeting tight junctions and transporters for vascular protection. *Am J Physiol Cell Physiol* **315**, C343–c356.

5 Yang C, Hawkins KE, Doré S and Candelario-Jalil E (2019) Neuroinflammatory mechanisms of blood-brain barrier damage in ischemic stroke. *Am J Physiol Cell Physiol* **316**, C135–c153.

6 Pugazhenthi S, Qin L and Reddy PH (2017) Common neurodegenerative pathways in obesity, diabetes, and Alzheimer's disease. *Biochim Biophys Acta* **1863**, 1037–1045.

7 Bertram S, Brixius K and Brinkmann C (2016) Exercise for the diabetic brain: how physical training may help prevent dementia and Alzheimer's disease in T2DM patients. *Endocrine* **53**, 350–363.

8 Brook E, Mamo J, Wong R, Al-Salami H, Falasca M, Lam V and Takechi R (2019) Blood-brain barrier disturbances in diabetes-associated dementia: Therapeutic potential for cannabinoids. *Pharmacol Res* **141**, 291–297.

9 Chakraborty S and Ain R (2017) Nitric-oxide synthase trafficking inducer is a pleiotropic regulator of endothelial cell function and signaling. *J Biol Chem* **292**, 6600–6620.

10 Wang Y, Cui L, Xu H, Liu S, Zhu F, Yan F, Shen S and Zhu M (2017) TRPV1 agonism inhibits endothelial cell inflammation via activation of eNOS/NO pathway. *Atherosclerosis* **260**, 13–19.

11 Icli B, Wu W, Ozdemir D, Li H, Cheng HS, Haemmig S, Liu X, Giatsidis G, Avci SN, Lee N *et al*, (2019) MicroRNA-615-5p regulates angiogenesis and tissue repair by targeting AKT/eNOS (Protein Kinase B/ Endothelial Nitric Oxide Synthase) signaling in endothelial cells. *Arterioscler Thromb Vasc Biol* **39**, 1458–1474.

12 Zhu Y, Xian X, Wang Z, Bi Y, Chen Q, Han X, Tang D and Chen R (2018) Research progress on the relationship between atherosclerosis and inflammation. *Biomolecules* **8**, 80.

13 Zhao B, Ren B, Guo R, Zhang W, Ma S, Yao Y, Yuan T, Liu Z and Liu X (2017) Supplementation of lycopene attenuates oxidative stress induced neuroinflammation and cognitive impairment via Nrf2/ NF-κB transcriptional pathway. *Food Chem Toxicol* **109**, 505–516.

14 Wang P and Miao CY (2015) NAMPT as a therapeutic target against stroke. *Trends Pharmacol Sci* **36**, 891–905.

15 Wang SN and Miao CY (2019) Targeting NAMPT as a therapeutic strategy against stroke. *Stroke Vascul Neurol* **4**, 83–89.

16 Ito S, Gotow T, Suetake I and Nagai K. (2020) Protective effects of nicotinamide mononucleotide against oxidative stress-induced PC12 cell death via mitochondrial enhancement. *J PharmaNutrition* **11**, 100175.

17 Chandrasekaran K, Choi J, Arvas MI, Salimian M, Singh S, Xu S, Gullapalli RP, Kristian T and Russell JW. (2020) Nicotinamide mononucleotide administration prevents experimental diabetes-induced cognitive impairment and loss of hippocampal neurons. *Int J Mol Sci* **21**, 3756.

18 Tarantini S, Valcarcel-Ares MN, Toth P, Yabluchanskiy A, Tucsek Z, Kiss T, Hertelendy P,

Kinter M, Ballabh P, Süle Z et al, (2019) Nicotinamide mononucleotide (NMN) supplementation rescues cerebromicrovascular endothelial function and neurovascular coupling responses and improves cognitive function in aged mice. Redox Biol 24, 101192.

19 Mateuszuk Ł, Campagna R, Kutryb-Zając B, Kuś K, Słominska EM, Smolenski RT and Chlopicki S (2020) Reversal of endothelial dysfunction by nicotinamide mononucleotide via extracellular conversion to nicotinamide riboside. Biochem Pharmacol 178, 114019.

20 Oita RC, Camp SM, Ma W, Ceco E, Harbeck M, Singleton P, Messana J, Sun X, Wang T and Garcia JGN (2018) Novel Mechanism for nicotinamide phosphoribosyltransferase inhibition of TNF-α-mediated apoptosis in human lung endothelial cells. Am J Respir Cell Mol Biol 59, 36–44.

21 Yabluchanskiy A, Ma Y, Iyer RP, Hall ME and Lindsey ML (2013) Matrix metalloproteinase-9: many shades of function in cardiovascular disease. Physiology (Bethesda, Md) 28, 391–403.

22 Zhong L, Simard MJ and Huot J (2018) Endothelial microRNAs regulating the NF-κB pathway and cell adhesion molecules during inflammation. FASEB J 32, 4070–4084.

23 Guerci B, Böhme P, Kearney-Schwartz A, Zannad F and Drouin P (2001) Endothelial dysfunction and type 2 diabetes. Part 2: altered endothelial function and the effects of treatments in type 2 diabetes mellitus. Diabetes Metab 27, 436–447.

24 van Sloten TT, Sedaghat S, Carnethon MR, Launer LJ and Stehouwer CDA (2020) Cerebral microvascular complications of type 2 diabetes: stroke, cognitive dysfunction, and depression. Lancet Diabet Endocrinol 8, 325–336.

25 Rochfort KD and Cummins PM (2015) The blood-brain barrier endothelium: a target for pro-inflammatory cytokines. Biochem Soc Trans 43, 702–706.

26 Chrissobolis S, Miller AA, Drummond GR, Kemp-Harper BK and Sobey CG (2011) Oxidative stress and endothelial dysfunction in cerebrovascular disease. Front Biosci (Landmark edition) 16, 1733–1745.

27 Sies H (2017) Hydrogen peroxide as a central redox signaling molecule in physiological oxidative stress: Oxidative eustress. Redox Biol 11, 613–619.

28 Yoshino J, Baur JA and Imai SI (2018) NAD(+) Intermediates: The biology and therapeutic potential of NMN and NR. Cell Metab 27, 513–528.

29 Kiss T, Nyúl-Tóth Á, Balasubramanian P, Tarantini S, Ahire C, Yabluchanskiy A, Csipo T, Farkas E, Wren JD, Garman L et al, (2020) Nicotinamide mononucleotide (NMN) supplementation promotes neurovascular rejuvenation in aged mice: transcriptional footprint of SIRT1 activation, mitochondrial

30 Kiss T, Balasubramanian P, Valcarcel-Ares MN, Tarantini S, Yabluchanskiy A, Csipo T, Lipecz A, Reglodi D, Zhang XA, Bari F et al, (2019) Nicotinamide mononucleotide (NMN) treatment attenuates oxidative stress and rescues angiogenic capacity in aged cerebromicrovascular endothelial cells: a potential mechanism for the prevention of vascular cognitive impairment. GeroScience 41, 619–630.

31 Caton PW, Kieswich J, Yaqoob MM, Holness MJ and Sugden MC (2011) Nicotinamide mononucleotide protects against pro-inflammatory cytokine-mediated impairment of mouse islet function. Diabetologia 54, 3083–3092.

32 Bhatt MP, Lim YC, Kim YM and Ha KS (2013) C-peptide activates AMPKα and prevents ROS-mediated mitochondrial fission and endothelial apoptosis in diabetes. Diabetes 62, 3851–3862.

33 Tezel G (2006) Oxidative stress in glaucomatous neurodegeneration: mechanisms and consequences. Prog Retin Eye Res 25, 490–513.

34 Song Y, Li S, Geng W, Luo R, Liu W, Tu J, Wang K, Kang L, Yin H, Wu X et al, (2018) Sirtuin 3-dependent mitochondrial redox homeostasis protects against AGEs-induced intervertebral disc degeneration. Redox Biol 19, 339–353.

35 Wang X, Hu X, Yang Y, Takata T and Sakurai T (2016) Nicotinamide mononucleotide protects against β-amyloid oligomer-induced cognitive impairment and neuronal death. Brain Res 1643, 1–9.

36 Rodríguez-Rodríguez A, Egea-Guerrero JJ, Murillo-Cabezas F and Carrillo-Vico A (2014) Oxidative stress in traumatic brain injury. Curr Med Chem 21, 1201–1211.

37 Liu C-Y, Bai K, Liu X-H, Zhang L-M and Yu G-R (2018) Hyperoside protects the blood-brain barrier from neurotoxicity of amyloid beta 1–42. Neural Regen Res 13, 1974–1980.

38 Gao J, Sana R, Calder V, Calonge M, Lee W, Wheeler LA and Stern ME (2013) Mitochondrial permeability transition pore in inflammatory apoptosis of human conjunctival epithelial cells and T cells: effect of cyclosporin A. Invest Ophthalmol Vis Sci 54, 4717–4733.

39 Bai M, Liu B, Peng M, Jia J, Fang X and Miao M (2019) Effect of Sargentodoxa cuneata total phenolic acids on focal cerebral ischemia reperfusion injury rats model. Saudi journal of biological sciences 26, 569–576.

40 Gentile C, Muise-Helmericks RC and Drake CJ (2013) VEGF-mediated phosphorylation of eNOS regulates angioblast and embryonic endothelial cell proliferation. Dev Biol 373, 163–175.

41 McMillin MA, Frampton GA, Seiwell AP, Patel NS, Jacobs AN and DeMorrow S (2015) TGFβ1 exacerbates blood-brain barrier permeability in a mouse

model of hepatic encephalopathy via upregulation of MMP9 and downregulation of claudin-5. *Lab Invest* **95**, 903–913.

42 Yao J, Shi Z, Ma X, Xu D and Ming G (2019) lncRNA GAS5/miR-223/NAMPT axis modulates the cell proliferation and senescence of endothelial progenitor cells through PI3K/AKT signaling. *J Cell Biochem* **120**, 14518–14530.

43 Wang P, Li WL, Liu JM and Miao CY (2016) NAMPT and NAMPT-controlled NAD metabolism in vascular repair. *J Cardiovasc Pharmacol* **67**, 474–481.